IOP Conf. Series: Materials Science and Engineering **278** (2017) 012136 doi:10.1088/1757-899X/278/1/012136

Modeling combined heat transfer in an all solid state optical cryocooler

Biju T Kuzhiveli

Centre for Advanced Studies in Cryogenics (CASC), National Institute of Technology Calicut, Calicut, India-673601

E-mail: btkuzhiveli@nitc.ac.in

Abstract. Attaining cooling effect by using laser induced anti-Stokes fluorescence in solids appears to have several advantages over conventional mechanical systems and has been the topic of recent analysis and experimental work. Using anti-Stokes fluorescence phenomenon to remove heat from a glass by pumping it with laser light, stands as a pronouncing physical basis for solid state cooling. Cryocooling by fluorescence is a feasible solution for obtaining compactness and reliability. It has a distinct niche in the family of small capacity cryocoolers and is undergoing a revolutionary advance. In pursuit of developing laser induced anti-Stokes fluorescent cryocooler, it is required to develop numerical tools that support the thermal design which could provide a thorough analysis of combined heat transfer mechanism within the cryocooler. The paper presents the details of numerical model developed for the cryocooler and the subsequent development of a computer program. The program has been used for the understanding of various heat transfer mechanisms and is being used for thermal design of components of an anti-Stokes fluorescent cryocooler.

1. Introduction

The possibility of cooling an object by making use of light was suggested as early as 1929 by Pringsheim[1]. After Landau[2] established the basic thermodynamic consistency of such a process, aspects of fluorescent cooling were vigorously pursued. However, attempts to cool solids with light have met with limited success due to the domination of unwanted heating effects. The breakthrough was made in 1995 with cooling of a solid as demonstrated by Epstein et al.[3] at Los Alamos National Laboratory(LANL) using Ytterbium doped Zirconium Fluoride glass (ZBLANP:Yb^3). Optical, solid state cryocooler has several advantages against mechanical coolers as they are rugged, vibration less, compact and free from electromagnetic interference thus offering years of life span with high efficiencies. The cooling powers are in principle comparable to current low capacity cryocoolers. It plays an important role in space cryogenics engineering because space based systems has been handicapped by absence of long term reliable compact cryogenic coolers. They are largely suitable for space based IR cameras, gamma ray spectrometers and electronics and also certain ground applications which demands about 80 K. Nevertheless, based on overall efficiency, they pose a greater disadvantage compared to mechanical coolers due to large unexpected losses. The low performance of the cryocooler is due to various spurious effects within the cryocooler and therefore a thorough thermal study was necessary.

2. Working principle

Optical refrigeration is based on absorbing light on the low energy side of a material absorption spectrum and re-emission at higher energies after equilibration with the thermal vibrations of the solid. Anti-Stokes fluorescence is the phenomenon by which a substance is excited by radiation at one wavelength ∼1060 to 1030nm and fluoresces at a shorter wave length typically ∼995nm. This results in more energy being radiated than is absorbed for each photon. A multi-watt laser is focused on to a nearly transparent material to accomplish this task.

3. Description of the optical cryocooler

Utilizing the above principle, by pumping a fluorescent cooling element with a high efficiency diode laser, a compact, all solid state optical cryocooler is envisaged for construction as shown in figure 1. The cooling element glass made with ZBLANP:Yb^3 hangs from the radiation shield. The radiation shield is cooled by thermoelectric coolers. The glass transmits cold to the cryotip through a transparent link. The cooling load is connected to the cryotip.

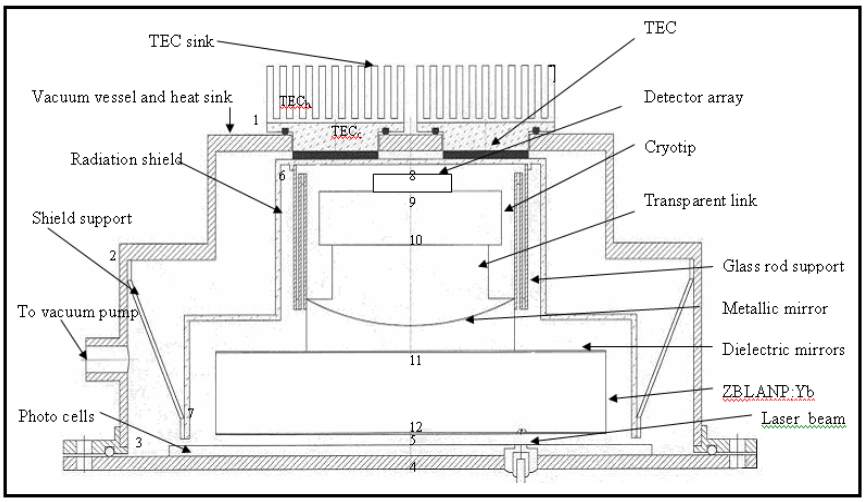

Figure 1. Optical cryocooler thermal network nodal points for two dimensional computational model.

4. Thermal network modeling

The equilibrium temperature of the sample is established by a balance between the laser induced fluorescent cooling and different heat loss mechanisms within the cryocooler, such as refrigeration and heat rejected by the thermoelectric coolers, heat radiation and convection to the environment and heat generation by escape radiation. Since the heating effects interact with the design parameters in different ways, a combined heat transfer simulation is required to predict the performance and to understand the design trade-offs involved. Therefore a thermal network model is developed which addresses all the radiative, convective and conductive heat transfer effects.

5. Procedure for finding out nodal temperatures based on the initial known conditions

In order to understand the refrigeration losses and heating due to escaped radiation, a network thermal model is envisaged by breaking the optical cryocooler system into different nodes. When the computational domain is discretized; x = mΔx and y = nΔy, where 'm' and 'n' are the number of 'x' and 'y' directional subdivisions, the mathematical equation are written in finite difference form as:

$$q_{i,j} = (T_{i+1,j} - 2T_{i,j} + T_{i-1,j})/(\Delta x)^2 + (T_{i,j+1} - 2T_{i,j} + T_{i,j-1})/(\Delta y)^2 = 0$$

To make the analysis computationally traceable, it is assumed that the components are rotationally symmetrical with respect to the 'y' axis. As a result, only half the section comes under the area of attention to be analyzed. The area is divided into many grids and the grid meeting points are considered as nodes. An energy balance is applied to each node, which results in an algebraic equation for the temperature at the node. By establishing energy balance, separate equations are derived for each node in the control volume which results into a combination of simultaneous differential equations and heat flux terms.

In addition to the conduction heat transfer, there are other forms of energy transfer encountered with the optical cryocooler. The combined heat transfer model accounts for the heat transfer mechanisms such as: (i) convection and radiation heat transfer from ambient to the wall of optical cooler or vice versa (ii) conduction heat transfer through the wall, shield support, support for optical material, transparent link, glues, thermal paste, cryotip, optical material, IR sensors and other sensors and heaters connected at various locations (iii) heat generated at various nodes, heat rejected by thermoelectric cooler (iv) refrigeration produced by optical material (ZBLANP:Yb^3) and cooling of radiation shields by the thermoelectric cooler (v) gaseous conduction inside the cryocooler chamber and natural convection outside the wall (vi) radiative heat transfer contribution within the cooler from each nodal area (vii) heat load due to sensor (viii) conduction heat transfer through the connecting wires used for sensors (mounted on the cryotip), ZBLANP:Yb^3 optical material and the heater at cryotip (ix) heat generated by the incipient laser beam.

By substituting for the heat transfer terms and by applying Kirchoff's current law analogy, for steady state conditions;

$$\Sigma q_{m-1} + \Sigma q_{other} = 0$$

Where Σq_{m-1} is the conduction heat flux from the surrounding nodes and 'm' is the number of surrounding nodes. Σq_{other} is the other heat flux terms arising out of convection, radiation, heat generation, refrigeration effect and heat rejected by thermoelectric coolers as appropriate.

When Fourier's law is applied to each of the grid lines for heat transfer by conduction, as an example; q_{2-1} = - k.$\Delta A \delta T/\delta x \approx$ k.$\Delta A(T_2\text{-}T_1)/\Delta x$ where the temperature gradient is evaluated at the mid plane between the two nodes and 'ΔL' is the depth of the two dimensional geometry measured. The accuracy by replacing the temperature gradient by the finite difference of two temperatures is not much sacrificed as the area under consideration is small.

The analysis for radiation network has assumed that each participating surface forming an enclosure is isothermal. In an attempt to satisfy this assumption, the surfaces which are not isothermal are divided into smaller areas until subdivided areas are reasonably isothermal. Applying an energy balance at node 1;

$$q_{TECh\_1} + q_{2\_1} + q_{TEC\_Rej} + q_{cout1} + q_{cin1} + q_{gen1} + q_{rout1} + q_{rin1} = 0$$

For the present 12 node system, similar equations are written down and the summarized equations are:

$$\Sigma q_1 = q_{TECh\_1} + q_{2\_1} + q_{TEC\_Rej} + q_{cout1} + q_{cin1} + q_{gen1} + q_{rout1} + q_{rin1} = 0$$
$$\Sigma q_2 = q_{1\_2} + q_{3\_2} + q_{7\_2} + q_{cout2} + q_{cin2} + q_{gen2} + q_{rout2} + q_{rin2} = 0$$
$$\Sigma q_3 = q_{2\_3} + q_{4\_3} + q_{cout3} + q_{cin3} + q_{gen3} + q_{rout3} + q_{rin3} = 0$$
$$\Sigma q_4 = q_{3\_4} + q_{5\_4} + q_{cout4} + q_{cin4} + q_{gen4} + q_{rout4} + q_{rin4} = 0$$
$$\Sigma q_5 = q_{4\_5} + q_{3\_5} + q_{cin5} + q_{cgen5} + q_{rin5} + q_{pcell} = 0$$
$$\Sigma q_6 = q_{TECc\_6} + q_{7\_6} + q_{10\_6} + q_{TEC\_Ref} + q_{cin6} + q_{gen6} + q_{r6} = 0$$
$$\Sigma q_7 = q_{2\_7} + q_{6\_7} + q_{cin6} + q_{gen7} + q_{rin7} = 0$$
$$\Sigma q_8 = q_{9\_8} + q_{sen} + q_{amb\_8} + q_{cin8} + q_{gen8} + q_{rin8} = 0$$
$$\Sigma q_9 = q_{8\_9} + q_{10\_9} + q_{cin9} + q_{gen9} + q_{rin9} = 0$$
$$\Sigma q_{10} = q_{6\_10} + q_{9\_10} + q_{11\_10} + q_{cin10} + q_{gen10} + q_{rin10} = 0$$
$$\Sigma q_{11} = q_{10\_11} + q_{om\_11} + q_{cin11} + q_{gen11} + q_{rin11} = 0$$

$$\Sigma q_{12} = q_{om\_12} + q_{T/c} + q_{om} + q_{las} + q_{cin12} + q_{gen12} + q_{rin12} = 0$$

where subscript 1 to 12 denotes nodal numbers, 'TECc'and 'TECh' are the refrigeration temperature produced by thermoelectric cooler, 'c' stands for convection, 'rad' for radiation 'in' for inner of the cryocooler volume and 'out' for outer of the cryocooler, 'gen' for heat generated, 'TEC' for thermoelectric cooler, 'Ref' for refrigeration, 'Rej' for heat rejected, 'pcell' for photocell, 'sen' for sensor, 'las' for laser heat, 'amb' for ambient, 'om' for the optical material ZBLANP:Yb^3.

For the first phase of numerical solution, the set of equations are solved based on the input boundary conditions (such as ambient conditions, thermoelectric cooler parameters: refrigeration capacity, thermoelectric cooler heat rejection, refrigeration produced by the ZBLANP:Yb^3, the optical material.) without the radiation heat fluxes included. Once the nodal temperatures are known the procedure for calculating radiative and convective terms are started.

By taking into consideration all the physical aspects, the generalized energy balance has been established and applied to each node which results into simultaneous differential equations. The result of the finite difference method for 'N' algebraic equation for 'N' nodes replaces the single partial differential equation and the applicable boundary conditions.

By determining the coefficients and constants of simultaneous equations the equations are arranged in the form as: $a_{11}T_1 + a_{12}T_2 + - - - + a_{1n}T_n = b_1$, where a_{ij} and b_i are input parameter based coefficients and constants respectively. T_i are the unknown temperatures. From this, the heat flux equations are organized as matrices, to determine the unknown parameters. The coefficient matrix 'A' is sparse and the constants in the equations are the elements that make up the column matrix 'B'. Set of equations are now condensed and be written with matrix notation as: AT = B, where 'T' is the temperature matrix. Since the values for a_{ij} and b_i are known, the calculation temperatures depend upon determining the inverse of matrix 'A'. The unknown nodal temperatures are given by equations of the form $T_1 = c_{11}b_1 + c_{12}b_1 + - - - + c_{1n}b_1$ (since $T_{(1-12)} = A^{-1}.B$), where c_{11}, c_{12},.....,c_{nn} are elements of the matrix 'C' ($C=A^{-1}$).

The elements of matrix 'A' and elements column matrix 'B' with nodal system for the given optical cryocooler are shown in table 1. For each node, the temperature is calculated with the physical properties of the material used. The inverse matrix is calculated by matrix inversion method which gives fairly good multiplication values ($AxA^{-1}=1$) with 12 nodes.

Table 1. Coefficient matrix corresponding to $T_{1-12}A(i,j)$ and constant matrix B(i).

T_1	T_2	T_3	T_4	T_5	T_6	T_7	T_8	T_9	T_{10}	T_{11}	T_{12}	B(i)
-a1	C1b	0	0	0	0	0	0	0	0	0	0	-Y1
C2a	-a2	C2b	0	0	0	C2c	0	0	0	0	0	-Y2
0	C3a	-a3	C3b	0	0	0	0	0	0	0	0	-Y3
0	0	C4a	-a4	C4b	0	0	0	0	0	0	0	-Y4
0	0	C5b	C5a	-a5	0	0	0	0	0	0	0	-Y5
0	0	0	0	0	-a22	C22b	0	0	C22c	0	0	-Y6
0	C26a	0	0	0	C26b	-a26	0	0	0	0	0	-Y7
0	0	0	0	0	0	0	-a61	C61a	0	0	0	-Y8
0	0	0	0	0	0	0	C62a	-a62	C62b	0	0	-Y9
0	0	0	0	0	C65a	0	0	C65b	-a65	C65c	0	-Y10
0	0	0	0	0	0	0	0	0	C66a	-a66	0	-Y11
0	0	0	0	0	0	0	0	0	0	0	-a70	-Y12

Once the temperatures of all the surfaces are now determined, the procedure for finding out the contribution made by radiation heat flux is carried out. By following a similar procedure, the desired net heat flux to all the surfaces can be determined.

6. Merging of numerical models, calculation procedure and computer program

In the first phase of the program the energy balance equation for each node is written down and solved for the temperatures. The input matrix used for calculating the primary nodal temperature is shown in table 2. All the units for the input file are in SI units except the geometrical parameters which are in mm. However, the program converts these values into SI units for calculation purpose.

Once the temperatures are obtained, it is necessary to obtain the radiation heat fluxes. The second phase of the program inputs the following files; shape factor matrix, emissivity matrix, physical properties and dimensions of cooler elements.

Input parameters in the table 2 is as follows: I^{st} row is the environmental parameters such as ambient temperature (K), natural convection coefficient over the heat sink (W/m^2K), the emissivity of heat sink, shape factor of heat sink, 2^{nd} row is starting temperature (K) to be used at different nodes, 3^{rd} row is thermoelectric cooler parameters (TEC) such as refrigeration temperature (K), heat rejection temperature (K), cooling power (W) and heat rejected (W), 4^{th} row is ZBLANP:Yb^3 optical material cooling temperature (K) and cooling power (W), 5^{th} row is the sensor load (W) which is connected to the cryotip, 6^{th} row is conductivities (W/mK) of different materials used, 7^{th} row is geometric parameters for Oring and thermal paste glue, 8-14^{th} rows are geometric parameters of the cryocooler (mm), 15^{th} row is heat generated (W) if any by escape radiation, 16-18^{th} rows are for the connecting wire parameters for number of wires used, thermal conductivity (W/mK), diameter (mm), length (mm), 19^{th} row is for internal vacuum parameters such as viscosity (Ns/m^2), density of gaseous matter (kg/m^3) in vacuum and specific heat ratio.

Table 2. Thermal, physical and geometrical parameters.

300.0,20.0,0.99,1.0
300.0,300.0,300.0,300.0,300.0,300.0,300.0,300.0,300.0,300.0,300.0,300.0
200.0,310.0,0.0,6.5
73.5,-0.62
0.4
8.0,300.0,200.0,120.0,10.0,5.0,8.0,6.0,120.0,200.0,30.0
22.0,13.0,0.2,21.0,5.0,0.1
2.0,2.0,11.2,2.0,1.2,10.5
2.75,2.0,2.5
5.0,31.0,45.0,53.0,43.0
20.75,34.5
5.0,14.0,12.0,16.0,30.0,36.7
8.0,14.75,11.25,9.0
3.0,4.0,4.0,4.0,6.0,0.75
0.0,0.0,0.0,0.0,0.0,0.0,0.0,0.0,0.0,0.0,0.0,0.0,0.0,0.0,0.0,0.0,0.0,0.0,0.0,0.0,0.0,0.0
2.0,71.0,0.19304,10.0
2.0,71.0,0.19304,10.0
2.0,71.0,0.19304,8.0
0.00001847,0.002,1.4

Since radiation shield forms two enclosures within the cryocooler inner volume, two matrices are formed. The first matrix consists of 7x7 shape factors and the second 8x8 shape factors. Since emissivities and shape factors could be different for external and internal surfaces of each participating nodal area, subscripts such as 'out' and 'in' are used to represent outer and inner

Table 3. Shape factor matrices F_{ij}(7,7) anf F_{ij}(8,8).

	j=1in	j=2in	j=3in	j=4in	j=5out	j=6out	j=7out	j=5in	j=6in	j=7in	j=8	j=9	j=10	j=11	j=12
i=1in	0.00	0.10	0.10	0.10	0.05	0.50	0.15	-	-	-	-	-	-	-	-
i=2in	0.10	0.00	0.00	0.10	0.10	0.10	0.60	-	-	-	-	-	-	-	-
i=3in	0.10	0.00	0.00	0.40	0.30	0.10	0.10	-	-	-	-	-	-	-	-
i=4in	0.10	0.10	0.40	0.00	0.30	0.10	0.00	-	-	-	-	-	-	-	-
i=5out	0.05	0.10	0.30	0.30	0.20	0.05	0.00	-	-	-	-	-	-	-	-
i=6out	0.50	0.10	0.10	0.10	0.05	0.00	0.15	-	-	-	-	-	-	-	-
i=7out	0.15	0.60	0.10	0.00	0.00	0.15	0.00	-	-	-	-	-	-	-	-
i=5in	-	-	-	-	-	-	-	0.00	0.00	0.20	0.00	0.00	0.00	0.00	0.80
i=6in	-	-	-	-	-	-	-	0.00	0.00	0.30	0.25	0.25	0.15	0.05	0.00
i=7in	-	-	-	-	-	-	-	0.20	0.30	0.00	0.00	0.00	0.00	0.25	0.25
i=8	-	-	-	-	-	-	-	0.00	0.25	0.00	0.00	0.75	0.00	0.00	0.00
i=9	-	-	-	-	-	-	-	0.00	0.25	0.00	0.75	0.00	0.00	0.00	0.00
i=10	-	-	-	-	-	-	-	0.00	0.15	0.00	0.00	0.00	0.00	0.65	0.20
i=11	-	-	-	-	-	-	-	0.00	0.05	0.25	0.00	0.00	0.65	0.00	0.05
i=12	-	-	-	-	-	-	-	0.50	0.00	0.25	0.00	0.00	0.20	0.05	0.00

nodal areas. For the first radiation enclosure, the participating nodes are: 1in, 2in, 3in, 4in, 5out, 6out, 7out. In the second enclosure, the participating nodes are designated as 5in, 6in, 7in, 8, 9, 10, 11, 12. Similarly two emissivity matrices are also formed. The shape factor matrices for the first and second enclosure are shown in table 3 and emissivity matrix in table 4.

Based on the preliminary nodal temperatures, the nodal radiation heat fluxes are determined which will provide all the necessary inputs for solving the set of equations and network problem completely.

Table 4. Emissivity matrices ϵ(1in-7out) and ϵ(5in-12).

ϵ(1in)	ϵ(2in)	ϵ(3in)	ϵ(4in)	ϵ(5out)	ϵ(6out)	ϵ(7out)
0.01	0.01	0.01	0.01	0.01	0.01	0.01

ϵ(5in)	ϵ(6in)	ϵ(7in)	ϵ(8)	ϵ(9)	ϵ(10)	ϵ(11)	ϵ(12)
0.01	0.01	0.01	0.01	0.01	0.01	0.01	0.01

Thus two individual numerical models for the components of the given thermal system are obtained and the models are merged to obtain an overall system solution. An iterative solution is carried out till a reasonable limit of precision is obtained.

A computer program is written to include computational model of the analysis. The amount of effort and time required to solve the simultaneous equation by conventional methods becomes large enough to warrant a computer solution.

7. Results

7.1. Effect of emissive properties

Initially it is assumed that the external surface of cooler body have highly reflective property (ϵ=0.01) and parts coming within the cooler body have near black body properties (ϵ=0.99). In order to find out the best emissive property for each member of the cryocooler, the emissivity of each surface is changed from the initial values. The different emisivities as applied to various surfaces are given in rows A, B, C, D, E, F in table 5. Wherever the surface have inner and outer surface exposed, the outer surface is denoted as 'Nout' and inner surface is denoted as 'Nin' where 'N' denotes the node number.

Effect of emissive properties of cryocooler sink external surface: As the emissivities are changed from conditions, A to B the heat radiated from the sink to ambient drastically improves. Changing to situations such as C, D, E slightly improves the heat radiated from external surface

Table 5. Emissivity of various cryocooler surfaces used for parametric study.

	1out	2out	3out	4out	1in	2in	3in	4in	5out	6out	7out	5in	6in	7in	8	9	10	11	12
A	0.01	0.01	0.01	0.01	0.99	0.99	0.99	0.99	0.99	0.99	0.99	0.99	0.99	0.99	0.99	0.99	0.99	0.99	0.99
B	0.99	0.99	0.99	0.99	0.99	0.99	0.99	0.99	0.99	0.99	0.99	0.99	0.99	0.99	0.99	0.99	0.99	0.99	0.99
C	0.99	0.99	0.99	0.99	0.01	0.01	0.01	0.01	0.01	0.99	0.99	0.99	0.99	0.99	0.99	0.99	0.99	0.99	0.99
D	0.99	0.99	0.99	0.99	0.01	0.01	0.01	0.01	0.01	0.01	0.01	0.99	0.99	0.99	0.99	0.99	0.99	0.99	0.99
E	0.99	0.99	0.99	0.99	0.01	0.01	0.01	0.01	0.01	0.01	0.01	0.01	0.01	0.01	0.99	0.99	0.99	0.99	0.99
F	0.99	0.99	0.99	0.99	0.01	0.01	0.01	0.01	0.01	0.01	0.01	0.01	0.01	0.01	0.01	0.01	0.01	0.01	0.01

of the sink thus concluding that the external surface must be coated with high emissivity material and all the interior surfaces with low emissivity material.

Effect of emissive properties of sink (inner surface) and outer area of photo cell plate: A similar study has been carried out to find out the influence of cryocooler sink inner surfaces. The conditions B and C generates spurious effects within the cryocooler envelop and are to be avoided.

Effect of emissive properties (outer of surface) of the radiation shield: It is seen that the radiation heat flux is reduced with low emissivity coating on the outer surfaces of radiation shield. It is recommended that condition B to be eliminated.

Effect of emissive properties of inner areas of photo cell plate, radiation shield inner surface and cooling assembly: As this is one of the critical areas of the cooler assembly special care is taken to see the effect of emissivity. The progress in reducing heat fluxes can be seen in figure 2. The best condition is obtained with an emissivity row 'E'.

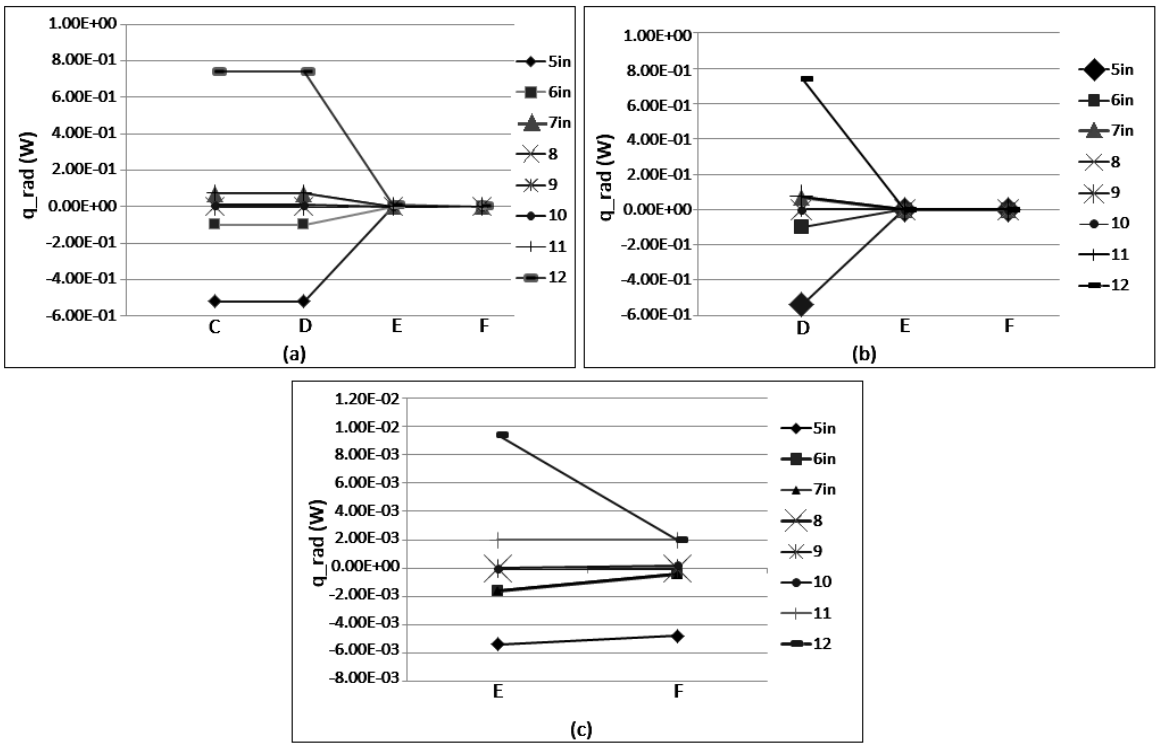

Figure 2. Effect of emissive properties of (a) inner areas of photo cell plate, (b) radiation shield inner surface and (c) cooling assembly.

7.2. Radiation flux dependence on radiation shield temperature cooled by thermoelectric cooler
For the study, the cooling temperature is changed from 200 K to 300 K. As expected the best result is obtained with the lowest temperature. The influence of radiation shield temperature on the radiation heat flux is shown in figure 3.

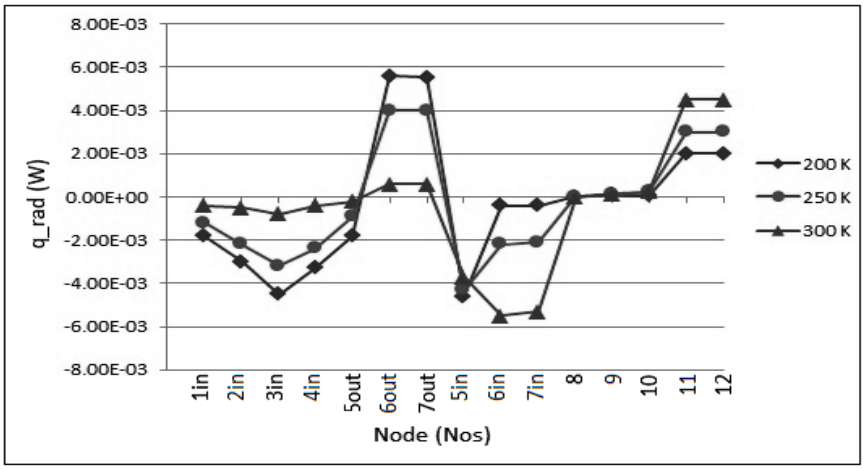

Figure 3.
Radiation flux dependence on radiation shield temperature cooled by thermoelectric cooler.

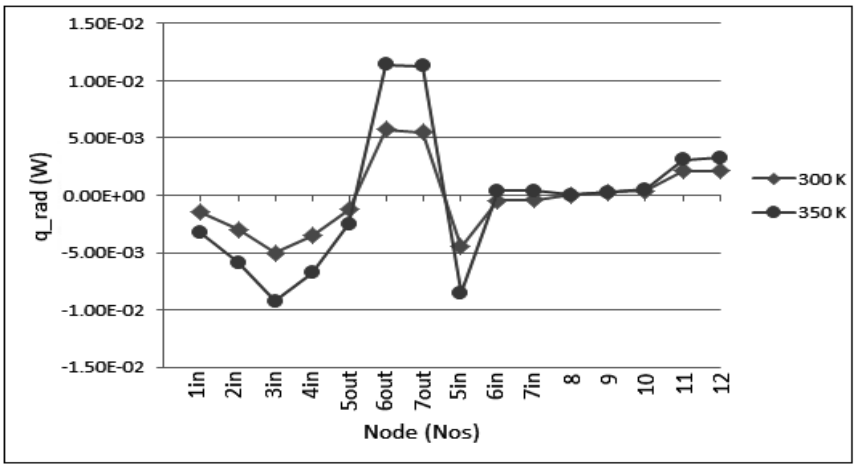

Figure 4.
Influence of ambient temperature on radiation heat flux.

7.3. Influence of ambient temperature on radiation heat flux
In figure 4, the influence of ambient temperature at 300 K and 350 K on the radiation heat flux is shown. It is worth noting that the enhanced ambient temperature has resulted in increased heat flux on the cooling material.

7.4. Effect of lead wires for sensor, heater
In the present configuration, three lead wires are used. One each is connected to the sensor and heater on the cryotip and the third one for a sensor fixed on the ZBLAN material. The effect of changing wire diameter from 0.19 mm to 0.5 mm on nodal temperature are presented in table 6. Usage of the increased diameter wire has resulted in 83.69 K from 77.29 K.

7.5. Influence of Temperature production on ZBLANP:Yb^3 material
The nodal temperature distribution for two ZBLAN optical material temperature is shown in table 7.

Table 6. Temperature on nodes for different lead wires.

Node(nos)	1	2	3	4	5	6	7	8	9	10	11	12
0.19mm wire	310.2	310	309.3	309.1	309	200	200.7	77.29	74.31	74.13	74.01	73.41
0.50mm wire	310.2	310	309.3	309.1	309	200	200.7	83.69	75.51	75.02	74.74	73.53

Table 7. Temperature on nodes for different ZBLANP:Yb^3 material temperature.

Node(nos)	1	2	3	4	5	6	7	8	9	10	11	12
at 73.5 K	310.2	310	309.3	309.1	309	200	200.7	77.29	74.31	74.13	74.01	73.41
at 100 K	310.2	310	309.3	309.1	309	200	200.7	103.6	100.8	100.6	100.5	99.91

8. Discussions and conclusion

Prediction of temperature distribution and radiant energy distribution in an optical cryocooler is one of the major inputs while designing the individual components of an optical cooler. In order to accomplish this, a thermal network computational model is envisaged using finite difference method, completed a numerical simulation of the optical cryocooler and is used to find out temperatures at various points and losses and intensity of radiant energy. Performance estimates of the device are presented based on the detailed thermal model. Details of the methodology for the heat transfer analysis program are also presented. The methodology developed is completely generic and can be applied to optical cryocooler of similar nature for solving temperature and radiant energy distribution of the cryocooler. The 230 inputable variable parameters includes dimensional parameters, physical properties, shape factors and emissivity. The governing equations are organized in a systematic fashion and thus results in a simple yet very powerful technique that can be used to analyze temperature distribution and radiation problems of this type. The thermal analysis program thus developed is well suited for parametric studies to recommend the dimensions and properties of the participating components and is thus helpful in designing the modules. A versatile, user friendly and powerful numerical technique along with a computer program has been developed involving radiative boundary, heat generation and heat absorption. It is observed that one dominant mode of radiation heat load is due to the emissivity of the participating surface. Since the problem has been solved for temperature distribution that includes internal heat generation/absorption under a variety of boundary conditions, the methodology is completely general. With the available thermal network model taking care of 230 input parameters is fully capable of describing all the modes of heat transfer mechanism in the cooler and will be also useful for thermal design of futuristic optical cryocoolers.

References

[1] Pringsheim P 1929 *Z. Phys.* **57** 739-746
[2] Landau L 1946 *J. Phys. Moscow* **10** 503-506
[3] Epstein R I et al. 1995 *Nature* **377** 500

Acknowledgments

Indian Institute of Science Bangalore entrusted consultancy work of thermal design of optical cryocooler to the author. Author greatly acknowledge the same.